JACS
JOURNAL OF THE AMERICAN CHEMICAL SOCIETY

Subscriber access provided by American Chemical Society

Article

A Mechanism for Transition-Metal Nanoparticle Self-Assembly

Claire Besson, Eric E. Finney, and Richard G. Finke

J. Am. Chem. Soc., **2005**, 127 (22), 8179-8184• DOI: 10.1021/ja0504439 • Publication Date (Web): 13 May 2005

Downloaded from http://pubs.acs.org on March 25, 2009

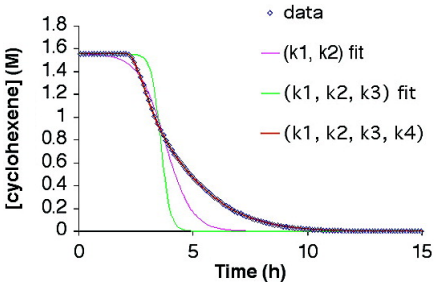

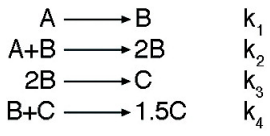

More About This Article

Additional resources and features associated with this article are available within the HTML version:

- Supporting Information
- Links to the 23 articles that cite this article, as of the time of this article download
- Access to high resolution figures
- Links to articles and content related to this article
- Copyright permission to reproduce figures and/or text from this article

View the Full Text HTML

ACS Publications
High quality. High impact.

Journal of the American Chemical Society is published by the American Chemical Society. 1155 Sixteenth Street N.W., Washington, DC 20036

J|A|C|S
ARTICLES
Published on Web 05/13/2005

A Mechanism for Transition-Metal Nanoparticle Self-Assembly

Claire Besson,§ Eric E. Finney, and Richard G. Finke*

Contribution from the Department of Chemistry, Colorado State University, Fort Collins, Colorado 80523

Received January 22, 2005; E-mail: rfinke@lamar.colostate.edu

Abstract: The four-step mechanism by which transition-metal nanoclusters or bulk-metal films self-assemble from metal salts under reductive conditions has been discovered. The presence of two autocatalytic steps in the same reaction scheme—double autocatalysis—is the key to the sharp "turn-on" feature after an induction period observed in the signature kinetic curves. Predictions of the new mechanism that are tested experimentally include the following: that low concentrations and high temperatures will favor nanoclusters over bulk-metal film formation; that bulk-metal is formed in some, if not many, literature syntheses reporting only Pt^0 nanoclusters; and that added ligands are one key to turning on the new mechanism. Particle-size-dependent metal-ligand bond dissociation energies are another implication from this mechanistic work.

Introduction

We have discovered the four-step mechanism by which transition-metal (TM) nanoclusters[1−6] nucleate, grow, and agglomerate—that is, self-assemble—under the commonly employed conditions of metal salt reductions. This mechanism, Scheme 1, explains previously inexplicable observations in the nanocluster literature and makes important predictions for the synthesis of TM nanoclusters and ligand effects on their catalysis. Transition-metal nanoclusters are of considerable current interest in many areas of modern science, for example, in catalysis,[1,2,5] photocatalysis,[7] and in optical,[8] electronic,[9] and magnetic[10] applications. The kinetics and mechanisms of self-assembly reactions are also of considerable current interest[11−14] but are nearly unknown[11,12] for systems as large and complex as the present example.

A comprehensive listing of the prior studies related to the mechanisms of transition-metal nanocluster formation and agglomeration is available in our prior mechanistic papers;[11,12] a few papers since then have also appeared.[15,16] However, only

Scheme 1

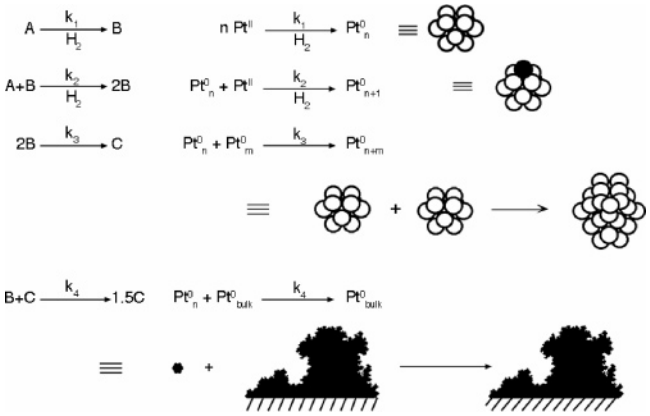

two prior papers exist on the kinetics and mechanism of transition-metal nanocluster formation and then agglomeration that are directly relevant to the present work and Scheme 1; the first (1997) paper details the *first two* steps of nanocluster formation[11] shown in Scheme 1, A → B, slow continuous nucleation, followed by an A + B → 2B autocatalytic surface growth, where A is a general organometallic precursor (such as (1,5-COD)$Pt^{II}Cl_2$ herein) and B is a nanocluster (e.g., Pt^0_n herein). Note that A + B → 2B is the kinetic definition of autocatalysis,[17] that is, where the product (B) is also a reactant, which means that the (autocatalytic) reaction proceeds faster and faster as the reaction progresses with, typically and in the prototype case,[11,12] a sigmoidal-shaped curve. Note also that once the fast A + B → 2B autocatalytic growth step turns on, it tends to consume the available A, thereby effectively shutting off the A → B nucleation step, thereby separating nucleation and growth in time[11,12] as needed to achieve near-monodisperse[4]

§ On leave from École Normale Supérieure, 45 rue d'Ulm, 75005 Paris, France as part of a six-month training course included in the second year of the Magistère de Chimie.

(1) Schmidt, G. *Chem. Rev.* **1992**, *92*, 1709.
(2) Bradley, J. S. In *Clusters and Colloids. From Theory to Applications*; Schmidt, G., Ed.; VHC: New York, 1994; pp 495−544.
(3) Schmidt, G.; Chi, L. F. *Adv. Mater.* **1998**, *10*, 515.
(4) Aiken, J. D., III; Finke, R. G. *J. Mol. Catal. A: Chem.* **1999**, *145*, 1.
(5) Widegren, J. A.; Finke, R. G. *J. Mol. Catal. A: Chem.* **2003**, *191*, 187.
(6) Finke, R. G. In *Metal Nanoparticles: Synthesis, Characterization, and Applications*; Feldheim, D. L., Foss, C. A., Jr., Eds.; Marcel Dekker: New York, 2001; Chapter 2.
(7) Brugger, P. A.; Cuendet, P.; Gratzel, M. *J. Am. Chem. Soc.* **1981**, *103*, 2923.
(8) Schon, G.; Simon, U. *Colloid Polym. Sci.* **1995**, *273*, 202.
(9) Ely, T. O.; Amiens, C.; Chaudret, B.; Snoeck, E.; Verelst, M.; Respaud, M.; Broto, J.-M. *Chem. Mater.* **1999**, *11*, 526.
(10) Thomas, J. M. *Pure Appl. Chem.* **1998**, *60*, 1517.
(11) Watzky, M. A.; Finke, R. G. *J. Am. Chem. Soc.* **1997**, *119*, 10382.
(12) Widegren, J. A.; Aiken, J. D., III; Öskar, S.; Finke, R. G. *Chem. Mater.* **2001**, *13*, 312.
(13) Fatin-Rouge, N.; Pfeil, S.; Rigualt, A.; Albrecht-Gary, A.-M.; Lehn, J.-M. *Helv. Chim. Acta* **2001**, *84*, 1694 and earlier papers in this series.
(14) Levin, M. D.; Stang, P. J. *J. Am. Chem. Soc.* **2000**, *122*, 7428.
(15) Tannenbaum, R. *Langmuir* **1997**, *13*, 5056.
(16) King, S.; Hyunh, K.; Tannenbaum, R. *J. Phys Chem. B* **2003**, *107*, 12097.
(17) Steinfeld, J. I.; Fransisco, J. S.; Hase, W. L. *Chemical Kinetics and Dynamics*; Prentice Hall: New Jersey, 1989.

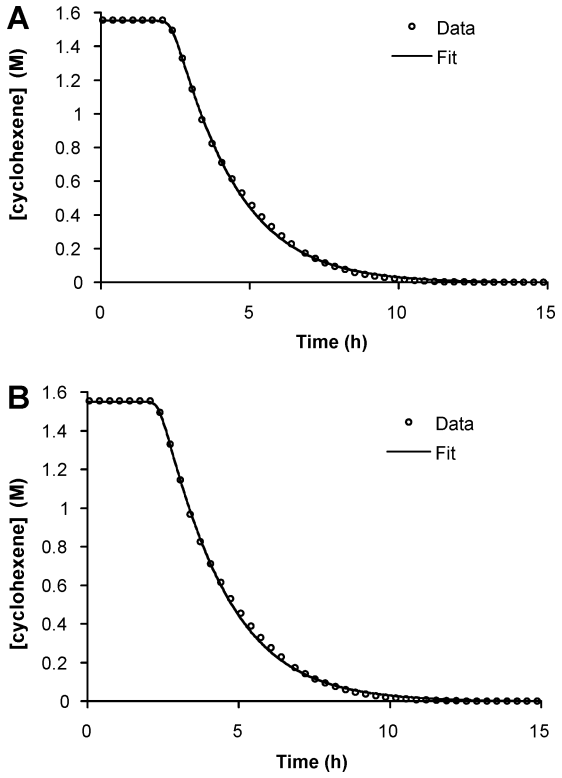

Figure 1. Standard cyclohexene hydrogenation curves. For clarity, only one out of every eight experimental points obtained is displayed. The curve-fits to double autocatalytic mechanism detailed in Scheme 1 are for different fourth steps of X + C → 1.5C, specifically X = A in Figure 1A and X = B in Figure 1B. The four rate constants for the MacKinetics grid-search-determined best fits[19] to the data (vide infra) in Figure A are $k_1 \sim 10^{-8}$ h^{-1}, $k_2 \approx 4.5$ M^{-1} h^{-1}, $k_3 \approx 10-35$ M^{-1} h^{-1}, and $k_4 \approx 0.7$ M^{-1} h^{-1}, and in Figure B, they are $k_1 \sim 10^{-7(\pm 4)}$ h^{-1}, $k_2 \approx 6 \pm 3$ M^{-1} h^{-1}, $k_3 = 0.69 \pm 0.04$ M^{-1} h^{-1}, and $k_4 = 0.16 \pm 0.03$ M^{-1} h^{-1}. The cited error bars for the Figure 1B data set come from 34 grid search curve-fits employing 34 different initial guesses for the k_1-k_4 parameters resulting in 34 visually good, R(residual) ≤ 0.01, fits[19] for this B + C → 1.5C fourth step of what turns out to be the proposed mechanism, vide infra.

nanoclusters. The second (2004) paper adds the *third step* to the mechanism,[18] a B + B → C agglomeration step (where C is bulk-metal).

The present work adds the new step of autocatalytic agglomeration of smaller nanocluster particles with larger, bulk-metal particles (B + C → 1.5C, rate constant k_4). The resulting four-step, novel *double autocatalytic step* mechanism is shown in Scheme 1.

Results and Discussion

Reaction Conditions, Products, Stoichiometry, and Kinetics. Our discovery began with the observation of the unprecedented kinetic curves shown in Figure 1—approaching step-function-like curves that have a ca. 0.4−3.0 h induction period, but which then "takeoff" *very suddenly* after that. The system underlying Figure 1 consists of 1.34 mM (1,5-COD)$Pt^{II}Cl_2$, 2.66 mM Bu_3N, 2.64 mM Proton Sponge (hereafter PS, which is 1,8-bis(dimethylamino)naphthalene, a strong, noncoordinating base used to scavenge the protons formed by H_2 reduction of Pt^{II}, Scheme 1), 1.65 M cyclohexene, and acetone as solvent (total volume 3 mL), all under 40 psig hydrogen. The reaction vessel is a culture tube placed in a 100 mL vortex stirred (via a stir bar and a magnetic stirrer) Fischer−Porter pressure-bottle reactor equipped with a computer-interfaced pressure transducer that can measure the loss of H_2 to ≤±0.01 psig. Curve-fits were accomplished using the GEAR/GIT numerical integration algorithm of MacKinetics.[19]

The clear, colorless reaction solution changes to a gray, then to a cloudy-black appearance (indicative of the formation of nanoclusters and suspended bulk-metal, vide infra) just after the end of the induction period. Transmission electron microscopy (TEM) of a drop of the solution harvested 5 min after the end of the induction period placed onto a Formvar-coated silicon−monoxide grid reveals the presence of 4.0 ± 1.0 nm nanoclusters (567 particles counted). At the end of the reaction, agglomerated black bulk Pt^0 metal (verified by XPS) is visible in the solution, on the stir bar and on the walls of the reaction tube; that is, a phase transition to bulk Pt^0 is occurring at the end of the induction period and when the reaction begins suddenly. The net Pt conversion reaction stoichiometry is that shown in eq 1.

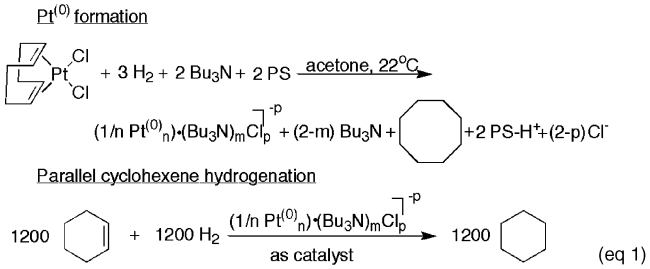

Phenomenologically, the overall reaction proceeds as if one forgot to add a reagent or to stir it until the reaction takes off; however, all of the required reagents are, in fact, present along with good stirring. The reactions are reproducible in their unusual shape and within the range of induction periods cited (which are known to be sensitive to the trace water and impurity content of the solvent,[20] as well as details of the stirring[21]). Note also that the way the reactions are being monitored indirectly, but powerfully and in real time, is via the relatively fast, catalytic, so-called pseudo-elementary step reporter reaction[11,12] of cyclohexene hydrogenation, the cyclohexene concentration being linked to the catalyst and precatalyst concentrations (Figure 2).

Arriving at the Proposed Mechanism by Ruling Out 15 Alternative Mechanisms. An exhaustive search of 15 alternative mechanisms reveals that only two mechanisms are able to fit the curve in Figure 1. A *second autocatalytic step*, specifically X + C → 1.5C (where X = A, Figure 1A or X = B, Figure 1B), added to our earlier, three-step mechanism,[11,18] is the key to being able to fit precisely the overall curve and its sudden "turn-on" feature, as the excellent curve-fits in Figure 1A,B demonstrate. Three of the 14 other alternative mechanisms considered and ruled out are shown in Figure 3A−C; the fits to the data are clearly inferior, hence, these mechanisms can be discarded. Significantly, in the case of Figure 1A,B, the kinetic curves can be fit *only when C, bulk-metal, is the catalyst*, an important point with additional implications to which we will

(18) Hornstein, B. J.; Finke, R. G. *Chem. Mater.* **2004**, *16*, 139 (addition/correction published in *Chem. Mater.* **2004**, *16*, 3972).

(19) MacKinetics, version 0.9.1b; Leipold, W. S., III. Information available on line at http://members.dca.net/leipold/mk/advert.html.

(20) Lin, Y.; Finke, R. G. *Inorg. Chem.* **1994**, *33*, 4891.

(21) Epstein, I. R. *Nature* **1995**, *374*, 321.

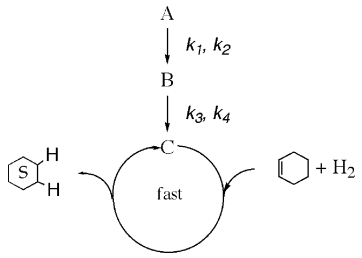

Figure 2. Simplified illustration of the fast, precedented "catalytic reporter" reaction of cyclohexene hydrogenation,[11,12] whereby the loss of H_2 or cyclohexene is used to follow the slower kinetics of conversion of (1,5-COD)$PtCl_2$ (A) into nanoclusters (B) which then agglomerate into bulk-metal (C), all dependent on four rate constants, k_1-k_4 (Scheme 1). In the present case, C is the active catalyst, and the figure illustrates the case where only the B + C → 1.5C (i.e., and not the A + C → 1.5C) step is kinetically important, as discussed further in the text.

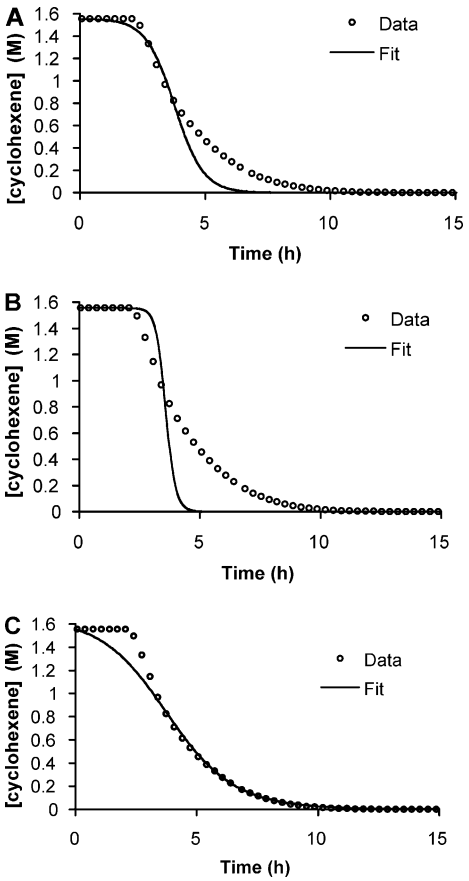

Figure 3. Standard hydrogenation curve showing the attempted curve-fits of 3 of 15 total alternative mechanisms that have been ruled out: (A) A → B, A + B → 2B with B as catalyst; (B) A → B, A + B → 2B, 2B → C with B as catalyst; (C) A → B, A + B → 2B, 2B → C, B + C → 1.5C with B as catalyst (i.e., in each case, B as catalyst for cyclohexene reduction as well as the conversion of A to B). For clarity, only one out of every eight experimental points obtained is displayed.

return in a moment. Equally excellent fits are obtained with either the B + C → 1.5C (Figure 1A) or A + C → 1.5C (Figure 1B) as the added, new step of the four-step mechanism (Scheme 1, vide infra).

However, the B + C → 1.5C mechanism is supported as the dominant kinetic path *under our conditions* on the basis of the following: TEM evidence (which reveals the presence of nanoclusters, B, on a sample taken 5 min after the induction period); numerical simulations (which show that only the B + C → 1.5C step allows the build-up of a significant amount of nanoclusters, B); synthetic experiments (which show that the present reaction can be tuned to yield only soluble nanoclusters rather than bulk-metal, vide infra); and loss of precursor, A, ^{1}H NMR and cyclooctane evolution (eq 1) GLC kinetic experiments. Those latter NMR and GLC kinetic experiments (analogous to the GLC experiments performed in our prior work (Figure 8 in ref 11) both verify the catalytic reporter reaction plus pseudo-elementary step method[11,12] used herein (Figure 2) and show that only the four-step mechanism with the B + C → 1.5C step (Scheme 1) can fit the NMR and GLC kinetic data. It seems likely, however, that the A + C → 1.5C step (i.e., the hydrogenation of precursor A to bulk-metal C via a surface autocatalytic growth step) will contribute kinetically in other cases, for example, when the alternative pathways that consume A (i.e., A → B and A + B → 2B) are kinetically slow.

We have also summarized in the Supporting Information the evidence which argues strongly against participation by soluble, homogeneous Pt(II) in response to the query of a reviewer. That evidence includes the complete poisoning of all the activity of a previously active catalyst by excess Hg^0 with good stirring, evidence that by itself argues strongly for Pt^0 as the only catalyst present (see the Supporting Information for experimental details).

Predictions, Further Experimental Tests of, and Important Insights from the Four-Step, Double Autocatalytic Mechanism. Any reliable new mechanism should be able to make predictions that can be tested experimentally; a truly new mechanism should also be able to explain previously inexplicable observations in the relevant literature. The following results demonstrate that these expectations are, in fact, the case for the mechanism in Scheme 1: (1) first, one main prediction of the mechanism is that lower concentrations and higher temperatures should favor nanocluster formation, B, over bulk-metal, C, since the k_1 step (and more nucleation leading to smaller nanoclusters) would be favored over the bimolecular steps, k_3 and k_4.

The above prediction proved almost "magic" in our hands. For the prior year, we had been trying to make near-monodisperse,[6] unagglomerated Pt^0_n nanoclusters following our $[M(COD)(solvate)_x]^+X^-$ and H_2 reduction method[22] and by surveying a range of anionic and other nanocluster stabilizers which included the premier polyanionic stabilizers[22] $P_2W_{15}Nb_3O_{64}^{9-}$ and HPO_4^{2-},[23] as well as Cl^-, Br^-, poly(vinylpyrrolidone), 1,10-phenanthroline, acetate, and their combinations along with the preferred higher dielectric, yet relatively weakly coordinating and thus nanocluster stabilizing, solvent propylene carbonate.[24,25] More than 100 synthetic survey experiments conducted over nearly a year *failed* under what proved to be the flawed reaction conditions of 1.2 mM (1,5-COD)$Pt^{II}Cl_2$ at 22.0 °C. In all cases, bulk Pt^0 metal resulted rather than the desired nanoclusters. This was initially a very surprising result since the literature strongly suggested (incorrectly, vide infra) that Pt^0 nanoclusters without bulk Pt^0 metal are easily prepared, especially since we were using premier nanocluster stabilizers and solvent. However, once the mechanism in Scheme 1 and its predictions became available, we were able to obtain Pt^0 nanoclusters stabilized by chloride in

(22) Özkar, S.; Finke, R. G. *J. Am. Chem. Soc* **2002**, *124*, 5796.
(23) Özkar, S.; Finke, R. G. *Langmuir* **2003**, *19*, 6247.
(24) Reetz, M. T.; Lohmer, G. *Chem. Commun.* **1996**, *16*, 1921.
(25) Hornstien, B. J.; Finke, R. G. *Chem. Mater.* **2003**, *15*, 899.

propylene carbonate *in a single, additional experiment* performed as follows (one successfully repeated five times since then): a 0.6 mM solution of (1,5-COD)$Pt^{II}Cl_2$ at 60.0 °C is reduced under 40 psig H_2 and in the presence of 2 equiv of Proton Sponge to yield well-formed 3.4 ± 1.0 nm nanoclusters. The predictions from the new mechanism, that lower concentrations and higher temperatures should favor nanoclusters over bulk-metal, proved strikingly true!

A second prediction of the mechanism is that Pt and other transition-metal nanocluster syntheses following the mechanism in Scheme 1 are generally not optimized and tend to produce bulk Pt^0 metal. Indeed, a search of >60 literature papers describing Pt^0 nanoclusters revealed that only four give an actual *yield* of nanoclusters, and even fewer report whether bulk-metal is made along with (or instead of) nanoclusters.[26,27] Hence, we devised a control experiment where we re-examined one of the most often cited preparations of Pt colloids, Hirai's preparation from a refluxing solution of $H_2PtCl_6 \cdot 6H_2O$ (0.6 mM) and 40 equiv of poly(vinylpyrrolidone) (average $M_w = 3500$) in a 1:1 mixture of methanol and water.[28] Repeating that often-cited preparation gave an unstable colloid solution that precipitated bulk-metal after 3 days. A second, repeat synthesis at the same concentration conditions (0.6 mM) but in pure methanol, plus employing our apparatus and cyclohexene hydrogenation reporter reaction kinetic methodology, gave a striking, step-function-like curve (not shown) that was well-fit by the mechanism in Scheme 1 plus the formation of *primarily bulk Pt^0 metal*, plus some nanoclusters (by TEM). A control reaction using 40 equiv of $M_w = 10\,000$ poly(vinylpyrrolidone) gave identical products and kinetics within experimental error to those using the smaller, average $M_w = 3500$ poly(vinylpyrrolidone). The observed step-function-like kinetic curve is of sufficient interest and importance (e.g., as an example of a chemical switch) that it is being investigated in greater detail and will be reported separately.[29]

Note that the above synthetic and kinetic results are consistent with, and in fact predicted by, the mechanism in Scheme 1. It is now clear that bulk-metal is a common contaminant in many preparations of Pt^0 nanoclusters in the literature; it is now also apparent why the yields of Pt^0 nanoclusters are rarely reported in the literature. Furthermore, it is now clear why higher (≥60 °C) temperatures are common in the four most successful syntheses. (It has been known for some time in semiconductor nanoclusters that higher temperatures favor the typically higher activation energy step of nucleation over growth and, therefore, narrower particle distributions.[30,31]) In short, the mechanism in Scheme 1 makes the prediction that most transition-metal nanocluster syntheses performed from metal salts under reductive conditions should survey lower concentrations and higher temperatures if nanoclusters are preferred, or the opposite conditions if deposition of a thin-metal film is the desired outcome.

A third, important implication from the mechanism in Scheme 1 follows from the finding that only if C bulk-metal is the active cyclohexene hydrogenation catalyst are we able to fit the observed kinetic data. That is, instead of the nanoclusters, B, being the most active catalysts as was typical previously,[5,11] the dominant catalyst is now the less energetic (i.e., more negative $\Delta H_{formation}$) and lower surface area bulk-metal. One is forced to the conclusion that the added Bu_3N and Cl^- ligands (L) have poisoned the nanoclusters—*but not the bulk-metal catalyst*. This, in turn, implies that bulk-metal-to-ligand (C−L) bond dissociation energies (BDEs) are weaker than those of the nanocluster-to-ligand (B−L) BDEs, a reasonable result given the nanocluster's more energetic (less negative $\Delta H_{formation}$), more electrophilic nature in comparison to that of their bulk-metal counterparts.[1−3,5,6] In short, particle-size-dependent metal-to-ligand BDEs are implied by our findings, at least as a working hypothesis meriting additional scrutiny.

A careful search of the literature reveals only one prior paper that does, however, provide independent, direct evidence for this little appreciated finding. That paper is Riley and co-workers' finding that Ni_n−nanocluster−N_2 BDEs are roughly *twice* those of bulk-metal−N_2 bond energies.[32] There is also other literature that supports in a general way the finding of higher M−L BDEs in nanoclusters versus those to bulk-metal. Schmid and co-workers' differential scanning calorimetry studies of $Au_{\sim 55}(PPh_3)_{\sim 12}Cl_{\sim 6}$ led them to conclude that "the Au−Au bonding (in the cluster) appears to be substantially stronger than in bulk gold".[33] The general observation that nanocluster surfaces are ca. 1−4% contracted versus the distances in bulk-metal[34] is also consistent with the electrophilic nature of the surface and the implied higher at least metal−metal, if not M−L, BDEs.

The finding of M−L BDEs that are greater in nanoclusters than in bulk-metal, and its implication of size-dependent nanocluster bond energies, has considerable ramifications for nanocluster and bulk-metal catalysis. One immediate implication is that the still relatively little explored area of nanocluster ligand effects may prove quite fruitful. More broadly, *size-dependent nanocluster bond energies could prove to be the most important, size-dependent property for catalysis to emerge from the nanocluster area*, if this working hypothesis holds up to the needed further testing.

Finally, a further prediction of the mechanism and its implied particle-size-dependent bond energies is that added ligands should be able to convert a system that showed only our two-step A → B, then A + B → 2B mechanism into one with the very sudden turn-on kinetics requiring the four-step mechanism, even when that system involves a different metal and ligands other than the above-studied Bu_3N or Cl^-. The results in Figure 4A,B confirm this prediction as well. Our standard Ir^0 nanocluster formation system with the premier polyanionic nanocluster stabilizer, the $P_2W_{15}Nb_3O_{62}$ polyoxometalate,[22] gives a standard sigmoidal curve fit by the two-step A → B, A + B → 2B mechanism[11] (Figure 4A). However, the addition of 44 equiv of pyridine completely changes the shape of the curve to one

(26) Moiseev, I. I.; Rudy, R. I.; Cherkashina, N. V.; Shubochkin, L. K.; Kochubey, D. I.; Novgorodov, B. N.; Kryukova, G. A.; Kolomiychuk, V. N.; Vargaftik, M. N. *Inorg. Chim. Acta* **1998**, *280*, 339.
(27) Rodriguez, A.; Amiens, C.; Chaudret, B.; Casanove, M.-J.; Lecante, P.; Bradley, J. S. *Chem. Mater.* **1996**, *8*, 1978.
(28) Hirai, H.; Nakao, Y.; Toshima, N. *J. Macromol. Sci. Chem.* **1979**, *A13*, 727.
(29) Finney, E. E.; Finke, R. G. Unpublished results and experiments in progress.
(30) Murry, C. B.; Norris, D. J.; Bawendi, M. G. *J. Am. Chem. Soc.* **1993**, *115*, 8706.
(31) Katari, J. E. B.; Colvin, V. L.; Alivisatos, A. P. *J. Phys. Chem.* **1994**, *98*, 4109.
(32) Parks, E. K.; Nieman, G. C.; Kerns, K. P.; Riley, S. J. *J. Chem. Phys.* **1998**, *108*, 3731.
(33) Benfield, R. E.; Creighton, J. A.; Eadon, D. G.; Schmid, G. *Z. Phys. D* **1989**, *12*, 533.
(34) Finke, R. G.; Özkar, S. *Coord. Chem. Rev.* **2004**, *248*, 135 and footnote 12 and references therein.

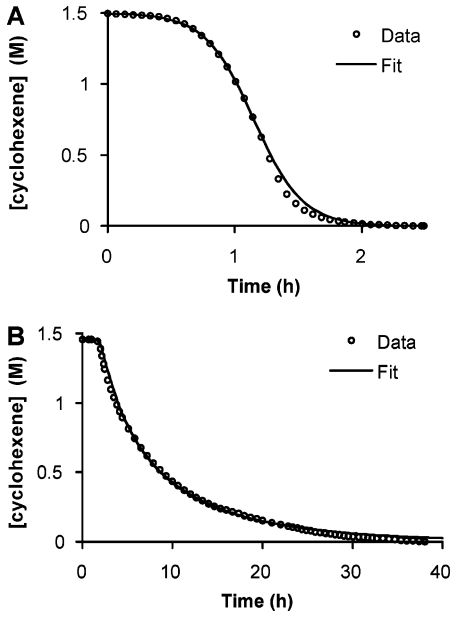

Figure 4. The cyclohexene hydrogenation reporter reaction curve for the cases of: (A) 1.3 mM $[Bu_4N]_8[1,5(COD)Ir{\cdot}P_2W_{15}Nb_3O_{62}]$, prepared in situ by the established route[22] of the addition of 1 equiv of $[Bu_4N]_9[P_2W_{15}O_{62}\text{-}Nb_3]$ to 1 equiv of $[(1,5\text{-COD})Ir(CH_3CN)_2]BF_4$ in propylene carbonate at 22 °C with 1.65 M cyclohexene and 40 psig initial H_2 pressure, but without added pyridine; and B the same as A except with 44 equiv of pyridine. For clarity, only one out of every four experimental points obtained in these particular experiments is displayed. Note the ca. 20-fold longer time scale of the *x*-axis in B versus A. The fit to the two-step mechanism for A yields $k_1 = 0.012$ h^{-1} and $k_2 = 4200$ M^{-1} h^{-1}, while the fit to the four-step mechanism in B yields $k_1 \sim 3 \times 10^{-3}$ h^{-1}, $k_2 \approx 3600$ M^{-1} h^{-1}, $k_3 \approx 85$ M^{-1} h^{-1}, and $k_4 \approx 240$ M^{-1} h^{-1}.

that requires the new, more general, four-step mechanism to fit that resultant kinetic curve (Figure 4B).

Unanswered Questions and, Hence, Important Goals for Future Research. The mechanism in Scheme 1 raises a number of interesting unanswered questions for future research. A few include the following. Exactly how general is the new mechanism in Scheme 1, and what are its limitations? What factors (different metals, ligands, concentrations, temperature, and so on) influence the new, self-assembly mechanism? Our just-begun survey (25 experiments at present while examining four different metals, two ligands, and two solvents as a function of different concentrations) suggests that the mechanism is more general (Ir, Rh, Ru, Pd, and Pt to date) but also indicates that a full understanding of all the factors that influence the mechanism in Scheme 1, with its double autocatalysis pathway, will require considerable additional research. Note that the fully detailed, intimate mechanism to even the relatively small 40 Å $Pt^0_{\sim 2200}$ particles observed must involve probably ≫2200 actual individual reaction steps represented by the four composite, pseudo-elementary steps[11] of Scheme 1. The effects of always-imperfect stirring[21] are one of the already established crucial factors in reactions with autocatalytic[21] steps; stirring effects should, therefore, be even more important in systems involving double autocatalysis. Another question is precisely how large are the agglomerates C? Back of the envelope calculations based on the fact that they are visible by eye implies a size of 0.1 mm (i.e., 0.003 rad when viewed at 25 cm[35]), corresponding to bulk crystalline platinum metal with a calculated *upper limit* of ca. 10^{11} atoms per particle. (Light-scattering experiments were considered but appear problematic due to the deposition of Pt^0 on the walls of any reaction vessel, such as a light-scattering cell.) Other important questions include: can a case be found where the A + C →1.5C step is kinetically dominant rather than the B + C → 1.5C step? What additional new *synthetic* insights, that is, beyond those demonstrated herein, can be achieved by the mechanistic insights provided by Scheme 1? Finally, can the k_3 and k_4 agglomeration rate constants be used to provide the first quantitative ranking scheme for the myriad of claimed nanocluster stabilizers that are currently appearing in the literature? (Other than a few recent papers,[22,23] prior ranking schemes are 35−100 years old, qualitative and applicable only to water soluble colloids,[36,37] not modern transition-metal nanoclusters.) The above are just a few of the important questions and interesting possibilities for additional research[29,38] raised by the transition-metal nanoparticle and bulk-metal self-assembly mechanism presented herein consisting of slow, continuous nucleation, autocatalytic surface growth, bimolecular agglomeration, and then autocatalytic agglomeration.

Experimental Section

General Considerations. Unless indicated otherwise, all commercially available solvents, compounds, and materials were used as received. Acetone, purchased from Burdick and Jackson (water content <0.2%), was purged with argon for at least 20 min before being stored in a nitrogen atmosphere drybox where it was used. The NMR solvent, CD_2Cl_2 (D, 99.9%), was purchased from Cambridge Isotope Laboratories. Cyclohexene (Aldrich, 99%) and tributylamine (J. T. Baker Chemicals) were both purified by distillation over sodium under argon and stored in the drybox. Hydrogen gas (General Air, 99.5%) was used as received. Dichloro-1,5-cyclooctadieneplatinum(II) ((1,5-COD)$PtCl_2$, 99%) was purchased from Strem Chemicals and stored in the drybox. Proton Sponge (1,8-bis(dimethylamino)naphthalene) (99%) was also stored in the drybox. Pyridine (Aldrich 99%) was distilled under vacuum and stored in the drybox over 4 Å activated molecular sieves. Poly(vinylpyrrolidone) (PVP, average M_w = 3500 and 10 000, K12) was purchased from Acros. Stock solutions of tributylamine and pyridine were prepared and stored in the drybox; the tributylamine solution (4.2×10^{-2} M) was prepared by mixing 0.1 mL of tributylamine and 9.9 mL of acetone; the pyridine solution (1.8×10^{-2} M) was prepared by adding 73 μL of pyridine to a volumetric flask and diluting to 50 mL with acetone. The Ir(0) nanocluster precursor, $(NBu_4)_5Na_3[(1,5\text{-COD})\text{-}Ir{\cdot}P_2W_{15}O_{62}Nb_3]$, was prepared according to our literature[39] and its purity checked by ^{31}P NMR.

Numerical integration curve-fitting is accomplished with MacKinetics, again all as detailed in our earlier papers[11,12,18] and elsewhere.[38]

Standard Conditions Hydrogenations with (1,5-COD)$PtCl_2$. A detailed description of the reaction apparatus and procedure is available in our 1997 and 2001 papers.[11,12] In the drybox, the precursor complex (1,5-COD)$PtCl_2$ (1.5 mg, 4.0 μmol) and 1.7 mg of Proton Sponge (8.0 μmol, 2 equiv) were weighed into a glass vial. To the vial was added 0.19 mL of a 0.0420 M solution of tributylamine in acetone (8.0 μmol, 2 equiv vs Pt) and 2.31 mL of acetone. The solution was mixed with a polyethylene pipet until it was homogeneous. Then the solution was transferred to a new 22 × 175 mm borosilicate culture tube that contained a new 15.9 × 9.1 mm Teflon-coated stir bar, and 0.5 mL of cyclohexene was added. The culture tube was placed into a 100 mL

(35) Welford, W. T. *Geometrical Optics*; Nord-Holland publishing Company: Amsterdam, 1962; p 115.
(36) Zsigmondy, R. Z. *Anal. Chem.* **1968**, *40*, 697.
(37) Thiele, H.; Van Levern, H. S. *J. Colloid Sci.* **1965**, *20*, 679.
(38) Besson, C.; Finney, E. E.; Finke, R. G. *Chem. Mater.*, **2005**, in press.
(39) (a) Hornstein, B. J.; Finke, R. G. *Inorg. Chem.* **2002**, *41*, 2720. (b) Pohl, M.; Lyon, D. K.; Mizuno, N.; Nomiya, K.; Finke, R. G. *Inorg. Chem.* **1995**, *34*, 1413.

Fischer−Porter bottle. The bottle was sealed, brought out of the drybox, and connected to the previously described apparatus[11] that is connected to a pressure transducer which, in turn, is interfaced to a computer running LabVIEW. The H_2 pressure loss is followed directly; this is then converted to the loss of cyclohexene from the known 1 H_2:1 cyclohexene catalytic reaction stoichiometry.

Standard Conditions Hydrogenation with $(NBu_4)_5Na_3[(1,5\text{-COD})\text{-}Ir\cdot P_2W_{15}Nb_3O_{62}]$. These reactions were carried out as described in our previous literature.[11,18]

Hydrogenation of $H_2PtCl_6\cdot 6H_20$. This reaction was performed as the ones above, using 1.0 mg of $H_2PtCl_6\cdot 6H_2O$ (1.9 μmol) and 8.6 mg of PVP (40 equiv vs Pt). The solids were dissolved in 2.50 mL of methanol. The temperature of the recirculating water bath[11] was set to 40 °C for the hydrogenation.

Acknowledgment. Support for this work was provided by DOE Grant DE-FG02-03ER15453 and NSF Grant 0314678 (for the research assistantship to C.B.). JoAn Hudson and her staff at the University of Oregon Microscopy Center are thanked for obtaining the reported TEMs. Lisa Starkey is acknowledged for performing the experiments reported in Figure 5, and colleagues Dr. Jason Widegren and Professors C. Michael Elliott and Elliot Bernstein at Colorado State University are thanked for reading and offering comments on an early version of the manuscript.

Supporting Information Available: The evidence against the main catalyst being some form of soluble, homogeneous Pt(II), including a Hg(0) poisoning experiment. This material is available free of charge via the Internet at http://pubs.acs.org.

JA0504439